Heat transfer and entropy generation for forced convection with CuO-water nanofluid

Mefteh Bouhalleb, Hassan Abbassi

Unit of Computational Fluid Dynamics and Transfer Phenomena,

National Engineering School of Sfax.BP1173,3038sfax, University of Sfax, TUNISIA

meftehbouhalleb@gmail.com

abbassihassen3@gmail.com

***Abstract*— The effects of nanofluid on laminar forced convection and entropy generated in a channel with a triangular obstacle set in the middle are investigated in the present paper by numerical methods. The numerical scheme is based on Control Finite-Element Method with the SIMPLER algorithm for pressure-velocity coupling. The fluid temperature at the channel inlet (T_c) is taken less than that of the walls (T_h). A wide spectrum of numerical simulations has been done over a range of Reynolds number, nanoparticles volume fraction and the aspect ratio. The influence of these parameters is investigated on the local and average Nusselt numbers and on the entropy generated. Numerical results, as obtained for CuO-water nanofluid, show that the inclusion of nanoparticles into the base fluid has produced considerable increases of generation entropy and the heat transfer. Also the results have also show that, in general, the heat transfer and entropy generated enhancement also increases considerably with an augmentation of the Reynolds number.**

Key words: nanofluid, entropy generated, heat transfer, forced convection, nanoparticles

I. INTRODUCTION

The forced convection heat transfer in a channel has relevance in many applications technologies, such as solar receivers exposed to wind currents, high performance boilers, nuclear reactors cooled during emergency shutdown, power plants, extrusion processes, glass fiber production and crystal growing [1-3]. Management of heat transfer for its enhancement or reduction in these systems is an essential task from an energy saving perspective [4-7].

Most traditional fluids, such as water, ethylene glycol, and oil, have limited heat transfer capabilities, which in turn, may impose severe restrictions in many thermal applications. So we must seek new strategies in order to improve the effective thermal behaviors of these fluids. With the progress in nanotechnology and thermal engineering, many efforts have been devoted to heat transfer enhancement. On the other hand, most solids, in particular metals, have thermal conductivities much higher compared to that of conventional fluids.

This is an era of emerging high heat flux devices such as computing chips, energy dense LASER applications, opto-electronics and super conducting magnets. The cooling requirements for these devices are enormous and require new strategies including the usage of new fluids. Suspending highly conducting solid particles in the coolant is one of the solutions to the above problem; however such slurries have a lot of practical limitations, primarily arising from the sedimentation of particles and the associated blockage issues. These limitations can be overcome by using suspensions of nanometer-sized particles (nanoparticles) in liquids, known as ‘nanofluids’.

Research on the thermal behavior of nanofluids has shown significant enhancement in heat transfer as compared to conventional slurries. Xie et al. [8] observed an enhancement of thermal conductivity up to 38% in the study for pump oil-based suspensions containing alumina particles with specific surface areas of 25 m2/g and at a volume fraction of 0.05. Assael et al. [9] investigated the enhancement of the thermal conductivity of water in the presence of carbon multiwall nanotubes. The thermal conductivity was measured with a transient hot-wire instrument built for this purpose, and operated with a standard uncertainty better than 2%.

Xue et al. [10] performed a nonequilibrium MD simulation to study how the ordering of the liquid at the liquid–solid interface affects the interfacial thermal resistance. They suggested that the experimentally observed large enhancement of thermal conductivity in suspensions of solid nanosized nanoparticles.

Improving the thermal conductivity is the key idea to improve the heat transfer characteristics of conventional fluids. It is a well known fact that metals in solid form have higher thermal conductivities than those of fluids. It has been shown in many references that, fluids containing suspended metal particles are expected to manifest significantly enhanced thermal conductivities relative to pure fluids [11-20]. The use of nanosize solid particles as an additive suspended into the base fluid (nanofluids) is a technique for the enhancement of heat transfer. Besides enhanced heat transfer, it is also found that the nanofluids eliminate most of the problems arising with micro size slurries like sedimentation, clogging of small channels, erosion, excessive pressure drop, etc. Thus, nanofluids have greater potential for heat transfer enhancement and are highly suited to application, in practical heat transfer processes.

The flow passing through a bluff body placed in the channel has been one of the most interested topics and occurs in many engineering applications such as the cooling of electronic components and heat exchangers. Enhancement of heat transfer by a bluff body placed in channel with devices leaves a topic of interest and has been investigated by researchers [21-26]. Wang et al.[23] reported that significance increase in heat transfer occurs as the flow becomes unsteady for a channel that has built in-line and staggered ribs. They reported that for an in-line case, the flow become unsteady at Reynolds number around 110 while for the staggered case this value is around 200. Mousa Farhadi et al [27] have studied numerically, the effect of wall proximity of a triangular obstacle on fluid flow and heat transfer in a horizontal plane channel. Results show that the vortex formation at the downstream of the obstacle has a main effect on the flow separation over the surface of the lower channelwall. Mohsen cheraghi et al [28], have studied the effect of cylinder proximity to the wall on channel flow heat transfer enhancement. The results show that the heat transfer increases from channel walls as a result of flow acceleration and vortex shedding phenomena.

Secondly Sasikumar and Balagi [29] have made a study for maximization heat transfer and minimization the heat transfer. The results show that, the greatest disadvantage of the entropy generated by the system is the reduction in the available energy of the system. Bejan [30] studied the effect of Reynolds number on the entropy generated. The made minimizing, gives an optimal Reynolds number where the entropy generated is minimal. Nag and Kumar [31] have performed a law optimization for a channel subjected to constant heat flux. They determined an optimum value of the initial temperature difference required for maintaining the entropy of the system at its minimum possible level.

II. GEOMETRICAL CONFIGURATION AND BOUNDARY CONDITIONS

In this study, the 2-D confined flow of an incompressible nanofluid in a channel with a built – in long equilateral triangular cylinder is investigated as shown in figure 1.

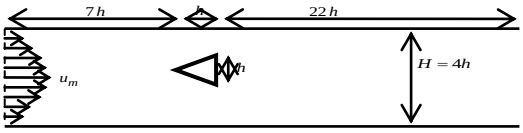

Fig.1 Schematics of the flow around a confined triangular cylinder.

The tow walls are at constant high temperature Th whereas the incoming flow is assumed to be in a constant low temperature Tc. The obstacle is supposed to be adiabatic, then doesn't contribute to any heat transfer and is exposed to a parabolic velocity field with maximum velocity Um. This practical situation is especially encountered in high performance boilers, cooling the blades of gas turbines.

Dimensionless boundary conditions are as follows:

At the channel inlet: $u = \frac{1}{4} y(4-y)$, $v = 0$ and $\theta = 0$

At the channel walls: $u = 0$, $v = 0$ and $\theta = 1$

At the channel exit: The Convective Boundary Condition (CBC) for u, v and θ is

used and the rate flow condition is imposed:

$$\int_0^4 u.dy = \frac{8}{3}$$

At the obstacle: u=0, v = 0, and the conduction equation is solved for θ imposing Neumann boundary condition at the walls: $\frac{\partial \theta}{\partial \boldsymbol{n}} = 0$, where n is the outward vector normal to the wall.

The convective boundary condition (CBC) is formulated as:

$$\frac{\partial \varphi}{\partial \tau} + u_{av} \frac{\partial \varphi}{\partial x} = 0 \quad (1)$$

Where φ = u, v or θ and uav is the average channel inlet velocity. As reported by Sani and Gresho [32] and Sohanker et al. [33], CBC predicts correctly the flow at the exit especially when vortices leave the domain. CBC allows vortices to smoothly pass away from the computational domain then, minimize the distortion of the vortices and reduce perturbations that reflect back into the domain.

III. GOVERNING EQUATIONS

For the 2-D incompressible flow, the non-dimensional forms of the continuity, the x-and y- components of momentum and energy equations may be expressed in the following form:

$$\frac{\partial U}{\partial X} + \frac{\partial V}{\partial Y} = 0 \quad (2)$$

$$\frac{\partial U}{\partial \tau} + U\frac{\partial U}{\partial X} + V\frac{\partial U}{\partial Y} = -\frac{\partial P}{\partial X} + \frac{\mu_{nf}}{\mu_f}\frac{\rho_f}{\rho_{nf}}\frac{1}{\mathrm{Re}_f}\left(\frac{\partial^2 U}{\partial X^2} + \frac{\partial^2 U}{\partial Y^2}\right) \quad (3)$$

$$\frac{\partial \theta}{\partial \tau} + U\frac{\partial \theta}{\partial X} + V\frac{\partial \theta}{\partial Y} = \frac{k_{nf}}{k_f}\frac{\rho_f}{\rho_{nf}}\frac{Cp_f}{Cp_{nf}}\frac{1}{\mathrm{Re}_f}\frac{1}{\mathrm{Pr}_f}\left(\frac{\partial^2 \theta}{\partial X^2} + \frac{\partial^2 \theta}{\partial Y^2}\right) \quad (4)$$

Where u , p and θ are the velocity, pressure, and temperature fields, respectively. Lengths are scaled by the square height h, pressure by ρnf×um2, where ρ is the fluid density and um is the peak inlet velocity, time by h/um and temperature by the imposed temperature difference between the walls and the incoming flow. Re and Pr are the usual Reynolds and Prandtl numbers.

The heat transfer performance is measured by space and time averaged Nusselt number which can be evaluated as:

$$Nu = \frac{k_{nf}}{k_f}\frac{1}{\tau_2 - \tau_2}\int_{\tau_1}^{\tau_2}\left(\int_0^{L/h} -\frac{\partial \theta}{\partial y} dx\right) d\tau \quad (5)$$

Where the time interval (τ2 - τ1) is the period of oscillations of the space averaged Nusselt number $\left(\int_0^{L/h} -\frac{\partial \theta}{\partial y} dx\right)$. The two integrals of equation (5) are numerically evaluated by the Simpson's method which is fourth order accurate.

The wake oscillation frequency fr is parameterized by the Strouhal number defined as:

$$st = \frac{fr\, h}{u_m} \quad (9)$$

IV. FORMULATION FOR ENTROPY CALCULATION

After obtaining the temperature distribution of the fluid flowing inside the channel and along the fins, the entropy generated by the system is calculated [34,35]. This consists of two parts (1) entropy generation due to heat transfer and (2) entropy generated due to fluid friction.

The local entropy generation resulting from heat transfer can be calculated as:

$$\dot{s}_h = \frac{k_{nf}}{k_f}\left[\left(\frac{\partial \theta}{\partial x}\right)^2 + \left(\frac{\partial \theta}{\partial y}\right)^2\right] \quad (10)$$

The entropy of the system due to fluid friction on account of pressure drop is determined by using Newton's law of viscosity in which we estimate the total power consumption from the shear stress developed and can be elucidated as follows:

$$\dot{s}_f = \varphi\left[2\left(\frac{\partial U}{\partial X}\right)^2 + 2\left(\frac{\partial U}{\partial Y}\right)^2 + \left(\frac{\partial U}{\partial Y} + \frac{\partial V}{\partial X}\right)^2\right] \quad (11)$$

$$\varphi = \frac{\mu_{nf}}{k_f} T_0 \left(\frac{\alpha_f}{H\Delta T}\right)^2 \quad (12)$$

The local total entropy is given by the follows expressing:

$$\dot{s}_T = \dot{s}_h + \dot{s}_f \quad (13)$$

The dimensionless total entropy generation is the integral over the system volume of the dimensionless local entropy generation:

$$s_T = \int_v \dot{s}_T \, \partial v \quad (14)$$

V. NUMERICAL METHODOLOGY

The combined continuity, momentum and energy equations are solved using a control volume finite element method adapted to the staggered grid. This method was inspired from the classic finite volume of Patankar [36] with some arrangements. The SIMPLER algorithm was applied to resolve the pressure–velocity coupling in conjunction with an Alternating Direction Implicit (ADI) scheme for performing the time evolution. When the conservation equation is integrated through the control volume, a Simpson method which is fourth order accurate in space has been used. More details about the numerical method and the validity of the computational code used in this work are available in Abbassi et al. [37] and Abbassi [38].

VI. RESULTS AND DISCUSSIONS

A. Grid independence and time step

To check the effect of grid spacing, computations have been performed for four different meshes with G1: 201 x 41, G2: 310 x 65, G3: 360 x 83 and G4:380x101 non uniform grids using the square cylinder for Re=100, Pr = 0.71 and d=1.5. Results concerning the Strouhal number St and averaged Nusselt number Nu values obtained with these different grids are tabulated in Table 1. The St and Nu values undergo a variation of 12.8% and 10.3% when we pass from G1 to G2 grid systems respectively

and 1.7%, 2.3% and 2.4 % when we pass from G2 to G3 grid systems respectively. Results given by G3 and G4 grids are close to each other. We can conclude that the G3 grid guarantees widely the independence of numerical results from the spacing mesh. In all the following study the G3 grid is used. The Strouhal number was found to be St =0.169 which is in the range of values St =0.165-0.170 found by the simulations of Sohankar et al. [36] for two-dimensional calculation of the square cylinder for various blockage and grid resolution parameters. It is also close to the value of St = 0.166 found by Mück et al. [39]. These results show the validity of the code used to achieve this study.

TABLE I GRID INDEPENDENCE STUDY. RE=100 AND D=1.5 FOR SQUARE CYLINDER.

Grid	G1: 201x41 $0.08 \leq \Delta x \leq 0.1$ $\Delta y = 0.1$	G2: 310x65 $0.0625 \leq \Delta x \leq 0.1$ $0.055 \leq \Delta y \leq 0.075$	G3: 360x83 $0.05 \leq \Delta x \leq 0.085$ $0.033 \leq \Delta y \leq 0.05$	G4: 380x101 $0.04 \leq \Delta x \leq 0.075$ $0.025 \leq \Delta y \leq 0.045$
St	0.1973	0.1720	0.1691	0.1638
Nu	1.2911	1.1582	1.1315	1.1307

B. *Effect of Reynolds number on the flow*

Figure 2 shows the structure of the flow in the vicinity of the long equilateral triangular obstacle for different Reynolds numbers varied from 40 to 140. The nanoparticles volume fraction is set to 1%.

For low Reynolds numbers, the viscous force dominates the flow here (fig 2a), the creeping steady flow past the obstacle triangular cylinder persists without separation. As the Reynolds number gradually increased, the magnitude of viscous forces decreases until a certain value (Re=60), at which the flow separates from the rear edge of the triangular obstacle and forms tow symmetrically placed vortices above and below the mid plane, that rotate in opposite directions, as shown in fig 2(b-e). This phenomenon, well known as the von karman vortex streets. Further increase the Reynolds number beyond the Rec, the oscillations in the wake grow in magnitude, and this state begins to shed vortices into the stream. For this study the critical Reynolds number is found to be Re=60.

(a)

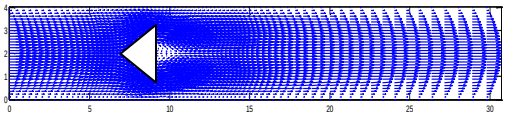

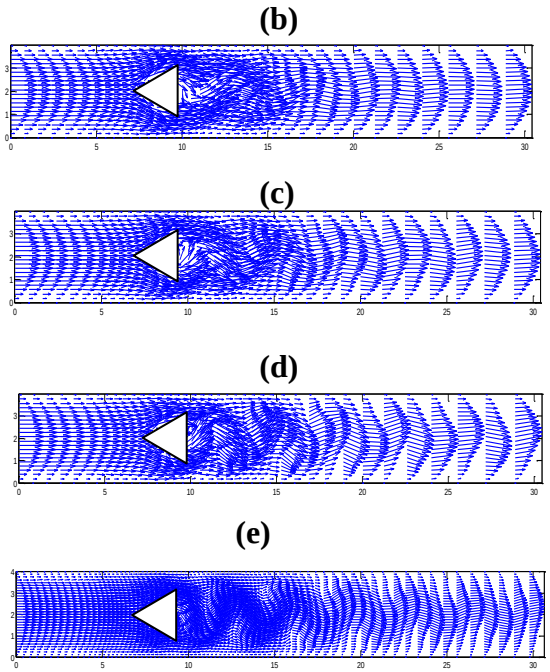

Fig 2. Instantaneous vorticity for different Reynolds number (a) Re=40, (b) Re=60, (c) Re=70, (d) Re=100 and (e) Re=140.

C. *Local Nusselt number*

Local bottom wall Nusselt number in the presence of the triangular cylinder obstacle for different Reynolds number and for varies nanoparticles volume fraction is shown in figure 3.

In the inlet region, a thermally developing flow exists, and all curves show nearly identical. For Re=40, the Nusselt number is very higher near y=0, decreases monotonically until reaching the obstacle, after attaining a maximum value it decreases in the far wake due to the effect of splitter after the obstacle. The addition of nanoparticles in the base fluid accelerates the nanofluid flow inside the channel. That why local Nusselt number increases with a nanoparticles volume fraction.

For Re=140, the effect of the presence of the obstacle is more important. The Nu curve is well disturbed, but appears floating above the dashed line because the vortex shedding after the triangular cylinder is unsteady. Secondary, peaks and crest further downstream occur and increases as a function of nanoparticles volume fraction.

An immediate conclusion can be made: the periodic flow increases with nanoparticles volume fraction increase, and promotes the heat transfer. This heat is diffused by the Von Karmen street vortex.

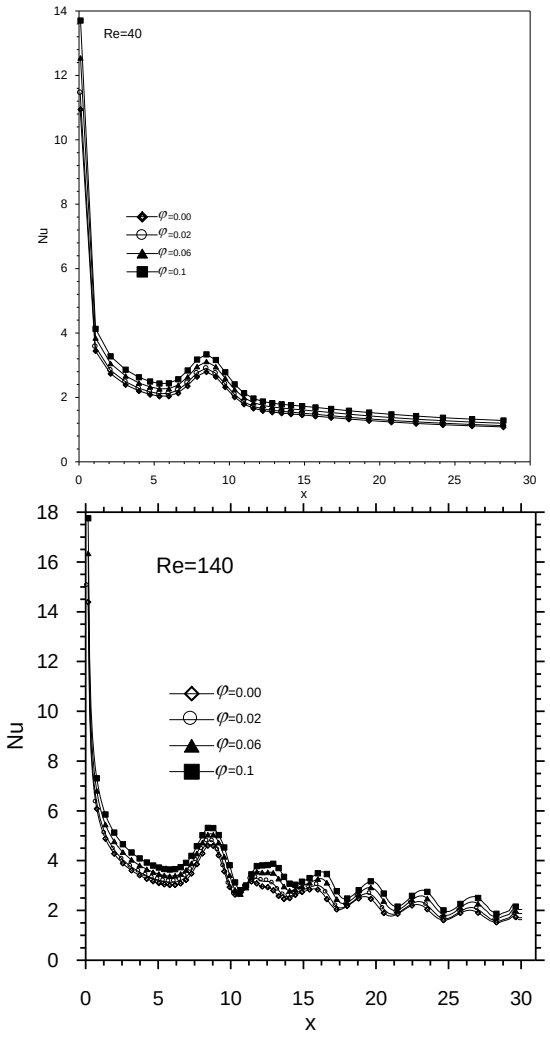

Fig. 3 Variation of the instantaneous Nusselt number, a function of nanoparticles volume fraction and for different Reynolds number.

D. Effect of the nanoparticles concentration on the average heat transfer

The influence of addition of nanoparticles in base fluid on the Nusselt number is show in figure 4. It can be seen that Nusselt number increases with the nanoparticles volume fraction. This implies that the amelioration of heat transfer rate, depends of nanoparticles and it increases with its volume fraction.

Therefore the dispersing, of CuO nanoparticles in the water can effectively increase the heat transfer even higher than that of the pure water. For instance, the heat transfer of suspension containing solid particles (10%), lead to a heat transfer enhancement of more than 18,2% in comparison with that of water.

We can notice here again similar behaviors regarding the influence of the Reynolds number (Re). The average Nusselt number has increased from 16% (Re=40), from 17% (Re=80) and from 18,2 (Re=140) for φ varying from 0% to 10%. We may see, here again, that the increase of Nu with respect to the parameter φ, become very pronounced for higher Reynolds number, say for Re=140.

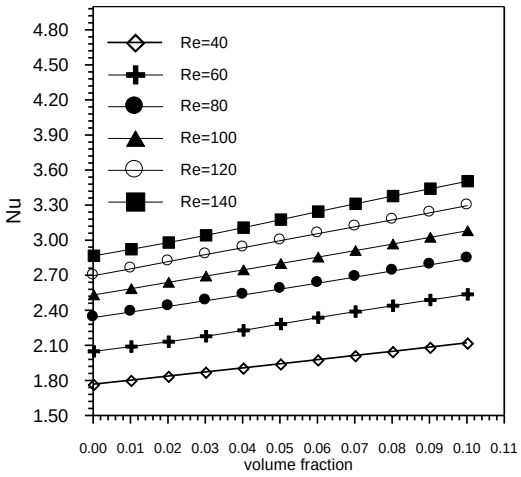

Fig. 4 Influence of parameter φ on average Nusselt number.

E. Effects of nanoparticles concentration on entropy generation

Figure 5 shows the variation of entropy generated by the system with nanoparticles volume fraction for different Reynolds number and as expected, it increases linearly with nanoparticles concentration.

The entropy generated has increased from 17.74% (Re=40), from 20.32 (Re=80) and from 20.52 (Re=140) for φ varying from 0% to 10%. So we can conclude that although the increase of nanoparticles volume fraction and Reynolds number increased the heat transfer, also yet it increased entropy generated. The greatest disadvantage of the

entropy generated by the system is the reduction in the available energy of the system.

For example, for (Re=40) and a nanoparticles concentration varied from 0% to 10%, the heat transfer is improved by 16%, whereas the entropy generated increases by 17%. Therefore the addition of nanoparticles in the base fluid (water) improves the heat transfer, but also increases the energy loss by the system.

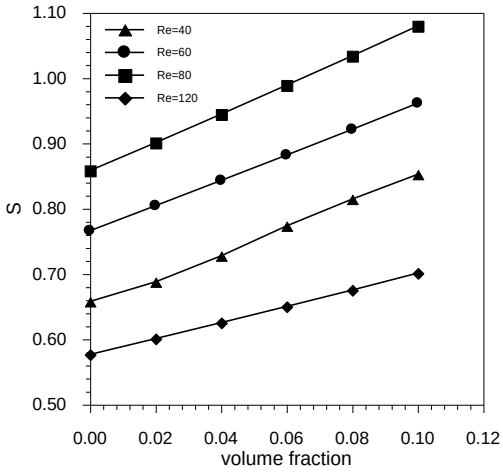

Fig.5 Variation of entropy generated by the system, with nanoparticules volume fraction, for different Reynolds number.

VII. CONCLUSIONS

The convective heat transfer performance and entropy generated of CuO-water nanofluid in a channel has been studied numerically. Simulation results have revealed that heat transfer increases as a result of flow acceleration and vortex shedding phenomena. The presence of nanoparticles increases the convective heat transfer coefficient and the entropy generated by 18.2% and 20% respectively than that of the original base fluid under the same Reynolds number. For the same volume fraction, it was found that as the Reynolds number increases, the heat transfer and the entropy generated increases.

In conclusion, this study has provided a clear insight into the thermal behavior of a nanofluid in a channel. I.e of the advantages and the disadvantages of the presence of nanoparticles, which increasing the heat transfer but increases the loss of energy by the system. The results found can easily be leveraged for various practical heat transfer and thermal applications to bring about a dynamic advancement in the field of nano scale heat transfer.

REFERENCES

[1] Fisher E. G., Extrusion of Plastics, Wiley, New York, 1976.

[2] Altan, T., Gegel, S. O. H., Metal Forming Fundamentals and Applications, American Society of Metals, Metals Park, OH, 1979.

[3] Tadmor, Z., Klein, I., Engineering Principles of Plasticating Extrusion, Polymer Science and Engineering Series, Van Nostrand Reinhold, New York, 1970.

[4] B.X. Wang, J.H. Du, X.F. Peng, Internal natural, forced and mixed convection in fluid-saturated porous medium, Transport Phenomena in Porous Media (1998) 357-382.

[5] Y. Demirel, H.H. Al-Ali, B.A. Abu-Al-Saud, Enhancement of convection heat transfer in a rectangular duct, Applied Energy 64 (1999) 441-451.

[6] K.C. Cheng, S.W. Hong, Effect of tube inclination on laminar convection in uniformly heated tubes for flat-plate solar collectors, Solar Energy 13 (1972) 363-371.

[7] O. Turgut, N. Onur, Three dimensional numerical and experimental study of forced convection heat transfer on solar collector surface, International Communications in Heat and Mass Transfer 36 (2009) 274-279.

[8] Xie H, Wang J, Xi T, Liu Y, Ai F, Wu Q Thermal conductivity enhancement of

suspensions containing alumina particles. J Appl Phys 91 (2002) :4568–4572.

[9] Assael MJ, Chen C-F, Metaxa I, Wakeham WA, Thermal conductivity of suspensions of carbon nanotubes in water. Int J Thermophys 25 (2004) :971–985.

[10] Xue L, Keblinski P, Phillpot SR, Choi SUS, Eastman JA, Effect of liquid layering at the liquid-solid interface on thermal transport. Int J Heat Mass Transf 47 (2004) :4277–4284.

[11] Liu, M.-S.; Lin, M.C.-C.; Huang, I-T.; Wang, C.-C. Enhancement of thermal conductivity with carbon nanotube for nanofluids. Int. Commun. Heat Mass Transfer 2005, 32, 1202-1210.

[12] Lee, S.; Choi, S.; Lee, S.; Eastman, J. Measuring thermal conductivity of fluids containing oxide nanoparticles. J. Heat Transfer 1999, 121, 280-289.

[13] Masuda, H.; Ebata, A.; Teramae, K.; Hishinuma, N. Alteration of thermal conductivity and viscosity of liquid by dispersion of ultra-fine particles. Netsu Bussei (Japan) 1993, 4, 227-233.

[14] Eastman, J.; Choi, S.; Li, S.; Yu, W.; Thompson, L. Anomalously increased effective thermal conductivities of ethylene glycol-based nanofluids containing copper nanoparticles. Appl. Phys. Lett. 2001, 78, 718-720.

[15] Xie, H.; Wang, T.; Xi, J.; Liu, Y.; Ai, F.; Wu, Q. Thermal conductivity enhancement of suspensions containing nanosized alumina particles. J. Appl. Phys. 2002, 91, 4568-4572.

[16] Das, S.; Putra, N.; Thiesen, P.; Roetzel, W. Temperature dependence of thermal conductivity enhancement for nanofluids. J. Heat Transfer 2003, 125, 567-574.

[17] Patel, H.; Das, S.; Sundararajan, T.; Sreekumaran, A.; George, B.; Pradeep, T. Thermal conductivities of naked and monolayer protected metal nanoparticle based nanofluids: Manifestation of anomalous enhancement and chemical effects. Appl. Phys. Lett. 2003, 83, 2931-2933.

[18] Choi, S.; Zhang, Z.; Yu, W.; Lockwood, F.; Grulke, E. Anomalously thermal conductivity enhancement of in nanotube suspensions. Appl. Phys. Lett. 2001, 79, 2252-2254.

[19] Xie, H.; Lee, H.; Youn, W.; Choi, M. Nanofluids containing multiwalled carbon nanotubes and their enhanced thermal conductivities. J. Appl. Phys. 2003, 94, 4967-4971.

[20] Choi, S.U.S. Enhancing thermal conductivity of fluids with nanoparticles, Developments and applications of non-Newtonian flows. ASME FED 231/MD, 1995, 66, 99-103.

[21] A.E. Bergles, Techniques to augment heat transfer, in: Handbook of Heat Transfer Applications. McGraw-Hill, New York, 1983, pp. 31-80.

[22] G. Biswas, H. Chattopadhyay, Heat transfer in a channel with built-in wing type vortex generators. Int. J. Heat Mass Transfer 35 (1992) 803-814.

[23] G. Wang, K. Stone, S.P. Vanka, Unsteady heat transfer in baffled channel. Heat and Mass Transfer 118 (1996) 585-591.

[24] A. Valencia, Numerical study of self-sustained oscillatory flows and heat transfer in channels with a tandem of transverse vortex generators. Heat and Mass Transfer 33 (1998) 465-470.

[25] H. Abbassi, S.B. Turki, S. Nasrallah, Numerical investigation of forced convection in a plane channel with a built-in triangular prism. Int. J. Thermal Sci. 40

(2001) 649-658.

[26] H. Chattopadhyay, Augmentation of heat transfer in a channel using a triangular prism. Int. J. Thermal Sci. 46 (2007) 501-505.

[27] Mousa Farhadi, Kurosh Sedighi, Afshin Mohsenzadeh Korayem, Effect of wall proximity on forced convection in a plane channel with a built-in triangular cylinder, International Journal of Thermal Sciences, 49 (2010) 1010-1018.

[28] Mohsen Cheraghi, Mehrdad Raisee, Mostafa Moghaddami, Effect of cylinder proximity to the wall on channel flow heat transfer enhancement, Comptes Rendus Mecanique.

[29] Sasikumar M, Balaji C Optimization of Convective fin systems: a holistic approach. Heat Mass Transfer 39 (2002): 57–68.

[30] Bejan A Second law analysis in heat transfer. Energy 5 (1980): 721–732.

[31] Nag PK, Kumar N Second law optimization of convective heat transfer through a duct with constant heat Flux. Int J Energy Res 13 (1989) :537–543.

[32] Sani RL,Gresho PM., Résumé and remarks on the open boundary condition minisymposium, In. J. Num. Meth. Fluids, vol.18, (1994) pp: 983-1008.

[33] Sohankar A, Norberg C, Davidson L., Low-Reynolds number flow around a square cylinder at incidence: Study of blockage, onset of vortex shedding and outlet boundary condition. In. J. Num. Meth. Fluids, vol.26, (1998) pp:39-56.

[34] A.C. Baytas, Optimization in an inclined enclosure for minimum entropy generation in natural convection, Int. J. Heat Mass Transfer 22 (1997) 145–155.

[35] A.C. Baytas, Entropy generation for natural convection in an inclined porous cavity, Int. J. Heat Mass Transfer 43 (2000) 2089–2099.

[36] Patankar S.V. (1980). Numerical Heat Transfer and Fluid Flow, Series in Computational Methods in Mechanics and Thermal Sciences, Hemisphere Publishing Corporation.

[37] Abbassi H, Turki S, Ben Nasrallah S., Numerical investigation of forced convection in a plane channel with a built-in triangular prism. Int. J. Thermal Sciences, vol. 40, (2001) pp: 649-658.

[38] Abbassi, H. 'Numerical analyses of the effect of Lorentz force on electrically conducting fluid flow around an obstacle. Progress in Computational Fluid Dynamics, vol. 12(6), (2012) pp.427–432.

[39] Mück B, Günther C, Müller U, Bühler L. (2000), Three-dimensional MHD flows in rectangular ducts with internal obstacles. J. Fluid Mechanics, vol. 418, pp: 265-295.

[40] A.K. De, A. Dalal, Numerical simulation of unconfined flow past a triangular cylinder, Int. J. Numer. Meth. Fluid. 52 (2006) 801–821.